Magnetic anisotropy and ferromagnetic correlations above the Curie temperature in Eu_2CuSi_3 single crystals

C. D. Cao,[1,2] R. Klingeler,[1,3] H. Vinzelberg,[1] N. Leps,[1] W. Löser,[1] G. Behr,[1] F. Muranyi,[1,4] V. Kataev,[1] and B. Büchner[1]
[1]*Leibniz-Institut für Festkörper- und Werkstoffforschung (IFW) Dresden, Postfach 270116, D-01171 Dresden, Germany*
[2]*Department of Applied Physics, Northwestern Polytechnical University, Xi'an 710072, People's Republic of China*
[3]*Kirchhoff Institute for Physics, University of Heidelberg, INF 227, D-69120 Heidelberg, Germany*
[4]*Physics Institute, University of Zürich, Winterthurerstr. 190, 8057 Zürich, Switzerland*
(Received 19 November 2009; revised manuscript received 19 July 2010; published 27 October 2010)

Magnetization $M(T,B)$, specific heat $c_p(T)$, and electrical resistivity $\rho(T,B)$ show ferromagnetic ordering in Eu_2CuSi_3 single crystals below the Curie temperature $T_C=34$ K. Temperature T and magnetic field B-dependent $M(T,B)$ data give evidence for a sizable magnetic anisotropy in the AlB_2-derived hexagonal structure at $T<T_C$. The increase in $|dM/dT|$ at T_C for $B=50$ mT along the easy magnetic c axis ($\langle 001\rangle$) is more than twice as large as for B along the a axis ($\langle 010\rangle$). The analysis of $c_p(T)$ in the magnetically ordered phase reveals signatures of a spin-reorientation process at $T\approx 10$ K below which the magnetic anisotropy in $M(T,B)$ almost vanishes. Measurements of electron-spin resonance (ESR) on Eu^{2+} ions reveal the anisotropy of the resonance field and the additional narrowing of the ESR signal at $T<100$ K that prove appreciable short-range ferromagnetic correlations far above T_C. These lead to a large negative magnetoresistance observed in the $\rho(T,B)$ measurements even up to a temperature $T\approx 100$ K. Below 50 K the ESR line starts to split due to the emergence of two magnetically nonequivalent Eu sites. The onset of magnetic order is manifested in the ESR spectrum by nucleation of a third line. Below $T\approx 10$ K, where thermodynamic data suggest a transformation of the ordered spins to a state with strongly reduced anisotropy, the ESR spectrum evolves into a featureless broad asymmetric peak.

DOI: 10.1103/PhysRevB.82.134446 PACS number(s): 75.50.Cc, 75.30.Gw, 75.47.De

I. INTRODUCTION

Magnetic properties of rare-earth (R) transition-metal (T) ternary intermetallic compounds have been a subject of intensive research. The great diversity of magnetic-ordering behavior observed originates from correlations of the localized f electrons of the rare-earth elements, which are coupled by the conduction electrons according to the Ruderman-Kittel-Kasuya-Yosida theory. Most compounds of the class R_2TSi_3 (T=Pd, Rh, Ni, Cu) exhibit a hexagonal AlB_2-type crystallographic structure and their interesting physical properties such as various types of magnetic ordering,[1–3] magnetoresistance anomalies,[4] and Kondo behavior[5,6] were revealed from polycrystalline samples. For Gd_2PdSi_3 a significant magnetocaloric effect was reported.[7] From single crystals grown by the tetra-arc Czochralski technique the anisotropy of transport and magnetic properties and metamagnetic transitions of Gd_2PdSi_3 (Ref. 8) and Ce_2PdSi_3 (Ref. 9) were deduced. Single-crystal growth of various R_2PdSi_3 compounds (R=Tb, Dy, Ce) by floating-zone (FZ) methods was described by Behr *et al.*[10] and Graw *et al.*[11] along with some details of their crystallization behavior. The anisotropy of transport and magnetic properties of FZ-grown single crystals of Tb_2PdSi_3,[12] Dy_2PdSi_3,[13] and Er_2PdSi_3 (Ref. 14) was reported. Tb_2PdSi_3 is a first example of substantial anisotropy of the magnetocaloric effect.[12] Frontzek *et al.*[15] provided a comprehensive analysis of the magnetocrystalline anisotropy in R_2PdSi_3 single crystals and discuss the competing effects of the crystal electric field and the magnetic two-ion interaction on the observed magnetic properties.

Among the lanthanides elemental europium is special because it has a half-filled $4f$ shell. Studies on Eu compounds are scarce due to the difficulties in controlling the Eu stoichiometry during sample preparation. The synthesis of Eu_2PdSi_3 and Eu_2CuSi_3, crystallizing in an AlB_2-type hexagonal structure, was first reported by Mallik *et al.*[3] and Majumdar *et al.*[4] Both show complex magnetic behavior of ferromagnetic type but Eu_2CuSi_3 exhibits a large negative magnetoresistance. In order to shed more light on magnetic-ordering behavior and intrinsic physical properties, measurements on single crystals are desirable. However, crystal growth so far was hampered by the volatile character of Eu. The applicability of floating-zone melting under elevated Ar pressure for crystal growth of the compound $EuCu_2Si_2$ with a lower melting temperature (1255 °C) than Eu_2CuSi_3 (1422 °C) was demonstrated only recently.[16,17]

Here, magnetic and electrical properties with particular respect to their dependence on the crystallographic orientation are studied on large single-crystalline samples from Eu_2CuSi_3 single crystals prepared by a floating-zone method. One special aim was local probing of the dynamic correlation of the magnetic ions by electron-spin resonance (ESR) measurements.

II. EXPERIMENTAL

The Eu_2CuSi_3 single crystal was grown by a vertical FZ technique with radiation heating in a vertical double ellipsoid optical configuration with a 5 kW air-cooled xenon lamp positioned at the focal point of the lower mirror.[16,18] For preparing feed rods high-purity elements Cu (99.999 wt %) and Si (99.9999 wt %) were first alloyed in an arc-melting furnace. Subsequently, Cu-Si and Eu (99.98 wt %) were comelted and cast to rods 6 mm in diam-

eter by a Hukin-type radio-frequency cold-crucible levitation melting equipment. A coarse-grained $Eu_{34.5}Cu_{15}Si_{50.5}$ seed and an $Eu_{34.3}Cu_{15}Si_{50.7}$ feed rod containing excess Eu with respect to the nominal Eu_2CuSi_3 ($Eu_{33.3}Cu_{16.7}Si_{50}$) stoichiometry to balance evaporation losses were utilized. The growth process proceeded with a velocity of 3 mm/h in a vacuum chamber under elevated pressure (5 MPa) of flowing Ar, in order to limit severe evaporation from the melt, which lead to deposits at the quartz walls of the growth chamber and reduce the light flux during the growth process. Bulk single crystals of Eu_2CuSi_3 were obtained, 6 mm in diameter and up to 15 mm length. The x-ray Laue backscattering method was utilized to check the quality and to determine the orientation of crystals. Microstructure and crystal perfection were examined by optical metallography and scanning electron microscopy.

Cuboids and rod-shaped specimens with a-axis ($\langle 010\rangle$) and c-axis ($\langle 001\rangle$) orientations within and perpendicular to the basal plane of the hexagonal unit cell, respectively, were all cut from one big crystal. Magnetization measurements were carried out in the temperature interval 2–300 K and in magnetic fields up to 5 T with a Quantum Design MPMS superconducting quantum interference device magnetometer. In addition, electrical resistivity (ρ) measurements were accomplished in a temperature range of 1.8–300 K and in the presence of magnetic fields up to 10 T in an Oxford magnet system by a conventional four probe method utilizing silver paint for contacting the leads with the sample. The specific heat was measured by means of a Quantum Design PPMS.

ESR experiments at the same cuboid specimen used for magnetic and specific-heat measurements, respectively, were performed with an X-Band Bruker spectrometer EMX series at a frequency $\nu=9.5$ GHz that was equipped with a He-gas flow cryostat for the variation in the sample temperature in the range 4–300 K.

III. RESULTS

A. Crystal structure

By the x-ray diffraction pattern it was ascertained that the present compound crystallizes in an AlB_2-derived hexagonal structure. The x-ray Laue backscattering image (Fig. 1) confirms the high perfection of the single crystal and the absence of defects such as secondary phases, disoriented grains or twinning. The preferred growth axis of the crystal rod deviates about 16° from crystallographic $\langle 100\rangle$ orientation within the basal plane of the hexagonal unit cell. From the powder x-ray diffraction pattern employing Cu $K\alpha$ radiation the lattice constants $a=4.0762$ Å and $c=4.4895$ Å were obtained, which are slightly different from the reported values of polycrystalline samples $a=4.095$ Å and $c=4.488$ Å.[4] A Cu-depleted composition 35.4 at. % Eu, 14.1 at. % Cu, and 50.5 at. % Si was determined by electron-beam microprobe analysis of the crystal. The different lattice constants seemingly originate in composition differences between the single crystal and polycrystalline samples due to the deviation of the homogeneity range of the intermetallic compound from the exact Eu_2CuSi_3 stoichiometry.

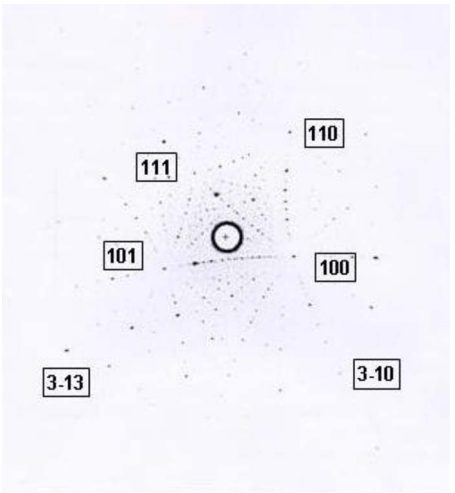

FIG. 1. (Color online) X-ray Laue backscattering image of the Eu_2CuSi_3 crystal with main reflections.

B. Static magnetization and specific heat

In Fig. 2, the magnetization is shown measured in a magnetic field of $B=50$ mT applied along the c axis, i.e., $B\|\langle 001\rangle$, and the a axis, i.e., $B\|\langle 010\rangle$, respectively. The most pronounced feature is the strong increase in the magnetization at low temperatures which implies the evolution of a spontaneous magnetic moment, i.e., the onset of ferromagnetic order at $T_C=34$ K. At high temperatures, the magnetization obeys a Curie-Weiss law as visible in the inverse static susceptibility B/M (inset of Fig. 2). Fitting of the data yields the ferromagnetic Weiss temperature $\theta=(34.5\pm0.5)$ K, i.e., there is an effective ferromagnetic coupling in agreement to the observed ferromagnetic order. Quantitatively, the effective magnetic moment $p_{\text{eff}}=(7.8\pm0.1)$ μ_B/Eu is derived from the data. This value agrees well to $p_{\text{eff}}=7.94$ μ_B which is expected for a free Eu^{2+} ion. The data hence provide strong evidence that the Eu ions exhibit the stable valence of 2+ in the temperature regime under study. Note that this

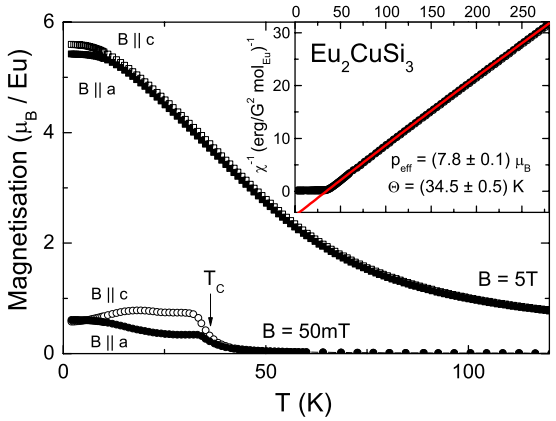

FIG. 2. (Color online) Magnetization of the Eu_2CuSi_3 crystal for two orientations of the external field $B\|a$ and $B\|c$, for $B=50$ mT and $B=5$ T, respectively. Inset: inverse magnetic susceptibility $\chi^{-1}=(M/B)^{-1}$ vs temperature, at $B=50$ mT. The straight line represents a Curie-Weiss fit (see the text).

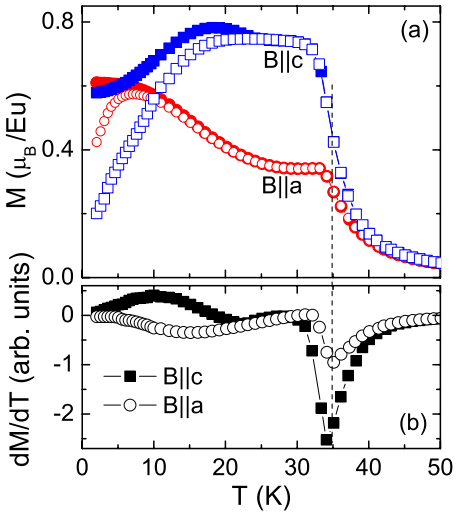

FIG. 3. (Color online) (a) Magnetization M for two orientations of the external field $B\|a$ and $B\|c$, at $B=50$ mT. Data have been taken both after field cooling (FC, filled symbols) and zero-field cooling (ZFC, open symbols). (b) Temperature derivative dM/dT of the FC data. The dashed line indicates the magnetic-ordering temperature T_C.

result is in contrast to findings for $EuCu_2Si_2$ where the effective valence is gradually reduced from ~2.84+ at 300 K to ~2.53+ at 50 K.[17]

The magnetization in the low-temperature ordered state exhibits additional features, which imply the complex nature of this phase. This becomes evident if the temperature dependence of the low-field magnetization and its derivative are considered (see Fig. 3). The data display a considerable anisotropy of the magnetic properties at T_C. The steep increase in magnetization $|dM/dT|$ along the easy magnetic c axis is more than twice as large as the slope along the a axis in the basal plane perpendicular to the c axis. At $T=30$ K the magnetization reaches 0.74 μ_B/Eu and 0.34 μ_B/Eu for external magnetic fields of 50 mT along the c axis and the a axis, respectively. In addition, beginning at $T\approx 25$ K the magnetization starts to rise again upon cooling for both orientations. Different from the monotonic behavior of $M(T)$ for the a axis the magnetization for the c axis decreases at $T<20$ K. As will be pointed out in more detail below, these changes most presumably indicate reorientation of spins in the ordered phase. Below 20 K, for $B\|c$, we also observe a small temperature hysteresis between field-cooled (FC) and zero-field-cooled (ZFC) data while a hysteresis for $B\|a$ is restricted to $T<10$ K. A small anisotropy of the magnetization is also visible at higher fields, i.e., at $B=5$ T (see Fig. 2). The temperature derivative dM/dT of the field-cooled magnetic data visualizes the ferromagnetic transition. The minimum indicates the magnetic-ordering temperature at $T_C=34$ K determined for the c axis, which slightly deviates from the a axis.

The field dependence of the magnetization $M(B)$ recorded at various constant temperatures confirms the observations described above. At $T=80$ K, the data imply paramagnetic behavior but typical ferromagneticlike curves are visible for low temperatures (Fig. 4). Again, the magnetization exhibits

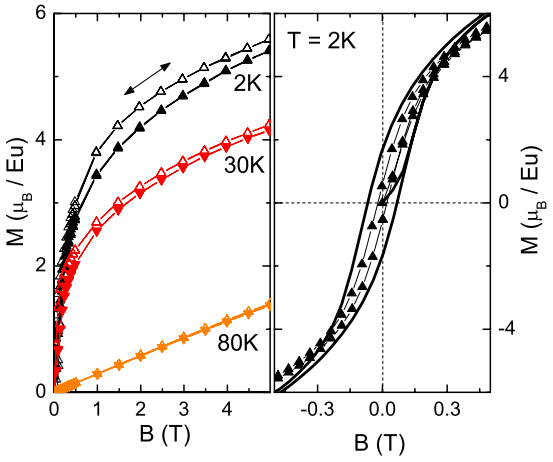

FIG. 4. (Color online) Magnetization of Eu_2CuSi_3 vs external magnetic field for $B\|a$ (filled symbols) and $B\|c$ (open symbols) at various temperatures. The low-field data for $B\|a$ (filled triangles) and $B\|c$ (bold line), at $T=2$ K, are shown on the right.

only small anisotropy in the ordered phase at $T=2$ K and there is a hysteresis at low temperatures. In agreement with the data in Fig. 3, the hysteresis loops for fields applied along the c axis are larger compared to those for the a-axis orientation.

The onset of magnetic order at T_C and additional changes at lower temperatures associated with spin reorientation are also visible in the specific-heat data shown in Fig. 5. The most pronounced feature is the jump at T_C which signals a second-order phase transition. Quantitatively, the jump in the specific heat amounts to $\Delta c_p \approx 9$ J/(mol K). Note that this value is considerably smaller than expected at the magnetic-ordering transition if a mean-field approach is applied, which predicts

$$\Delta c_p = \frac{5Nk_B}{2}\frac{(2J+1)^2-1}{(2J+1)^2+1} \approx 40.3 \text{ J/(mol K)}.$$

We therefore conclude the presence of either strong magnetic disorder below T_C or considerable short-range magnetic or-

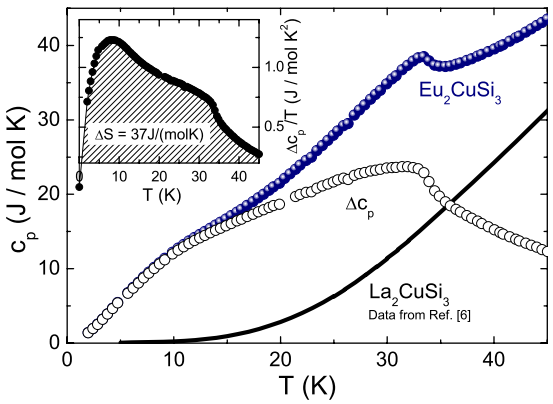

FIG. 5. (Color online) Specific heat as function of temperature of Eu_2CuSi_3 (filled circles) and La_2CuSi_3 (line, from Ref. 6). The difference Δc_p between these two data sets represented by the open circles estimates the magnetic contribution to the specific heat of Eu_2CuSi_3. Inset: $\Delta c_p/T$ vs T.

der at higher temperatures (cf., e.g., Ref. 19) as presumed by Majumdar *et al.*[4]

In addition to the pronounced signature of the magnetic phase transition at T_C, there is a broad hump in the specific-heat data around $T=10$ K. This broad anomaly indicates that the changes in the magnetization in the ordered phase are associated with anomalous entropy changes, too. For a quantitative estimate, we have subtracted the specific heat of the isomorphic nonmagnetic counterpart of Eu_2CuSi_3, i.e., La_2CuSi_3 (data taken from Ref. 6), from our data. We assume that the specific heat of the isostructural compound La_2CuSi_3 provides an estimate for the pure phononic specific heat. Note that the data for La_2CuSi_3 have been scaled by a factor of 1.046. This correction to the lattice contribution takes into account the different masses of the La and Eu atoms. Subtraction of the data indicates significant magnetic entropy changes above the magnetic-ordering temperature T_C. The magnetic entropy changes in the accessible temperature range up to 45 K, which are calculated according to this analysis, amount to ~37 J/(mol K). Although our analysis overestimates the magnetic entropy changes, this value fairly agrees to the total magnetic entropy associated with ordering of the Eu^{2+} moments, i.e., $\Delta S_{magn}=R\ln(2S+1)\approx 34.6$ J/(mol K). In general, the analysis of the specific heat implies (1) magnetic fluctuations in the paramagnetic regime and (2) significant magnetic disorder at T_C, which persists down to relatively low temperatures.

C. ESR measurements

A well-defined ESR response has been detected from the sample in the entire temperature range of the study ($T=4-300$ K). For the presentation of the data it is useful to define two temperature regimes: A high-T (HT) regime above ~50 K, and a low-T (LT) regime below ~50 K. At HT the ESR spectrum comprises a single line of an asymmetric shape, typical for the ESR of localized magnetic moments in a metal (Fig. 6, inset). It can be perfectly fitted with the so-called Dysonian line profile,[20] which yields the values of the resonance field B_{res}, the linewidth ΔB and the intensity of the signal. The position of the line corresponds to the g factor $g\approx 1.96$, which is very close to a spin-only value of 2 and only slightly depends on the direction of the external magnetic field relative to the crystallographic c axis of the sample (see below). This g-factor value is characteristic for the Eu^{2+} ion, which possesses the spin moment only ($S=7/2$, $L=0$).[21] The occurrence of a well-defined ESR signal evidences a stable 2+ valence state of Eu in Eu_2CuSi_3, since even a small broadening of the $4f$ level due to charge fluctuations would make ESR of Eu unobservable (see, e.g., Ref. 22).

Generally, the intensity of the ESR signal is proportional to the static susceptibility of the spins participating in the resonance. For Eu_2CuSi_3 in the HT regime it closely follows the Curie-Weiss law (Fig. 6). The corresponding fit yields the values of the paramagnetic Curie temperature $\theta_p^{ESR}=29$ K and the ferromagnetic ordering temperature $T_C^{ESR}=31$ K, which are very similar to the estimates of θ_p and T_C from the static magnetization measurements at the same sample (see Sec. III B). This similarity enables to conclude that ESR probes the same Eu spins which contribute to static magnetic properties.

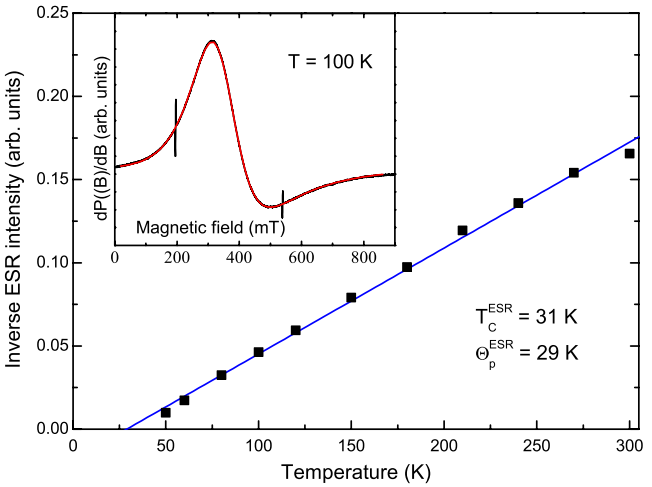

FIG. 6. (Color online) Inset: ESR signal [field derivative of the microwave absorption $dP(B)/dB$ from Eu_2CuSi_3 at $T=100$ K] together with the Dysonian fit. The experimental line and the fit are indistinguishable in the plot. Sharp resonances are due to field markers. Main panel: T dependence of the inverse intensity of the ESR signals (squares). The solid line is a fit to the Curie-Weiss law which yields the ESR estimate of the paramagnetic Curie temperature $\theta_p^{ESR}=29$ K and the ferromagnetic ordering temperature $T_C^{ESR}=31$ K.

In the HT region the resonance field is almost T independent and begins to shift to somewhat lower values by approaching a temperature of 50 K [Fig. 7(a)]. The linewidth, however, exhibits an appreciable T dependence [Fig. 7(b)].

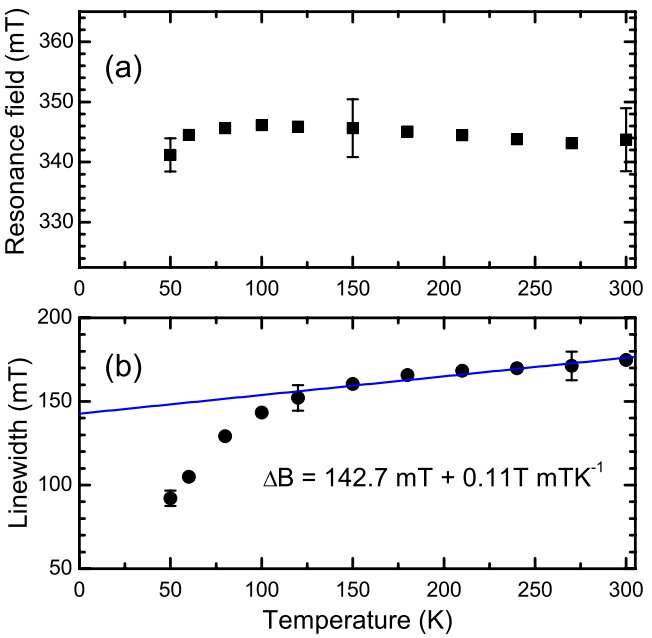

FIG. 7. (Color online) Temperature dependence (a) of the ESR resonance field B_{res} and (b) of the linewidth ΔB for a magnetic field parallel to the c axis. The solid line in (b) is a linear Korringa fit (see the text).

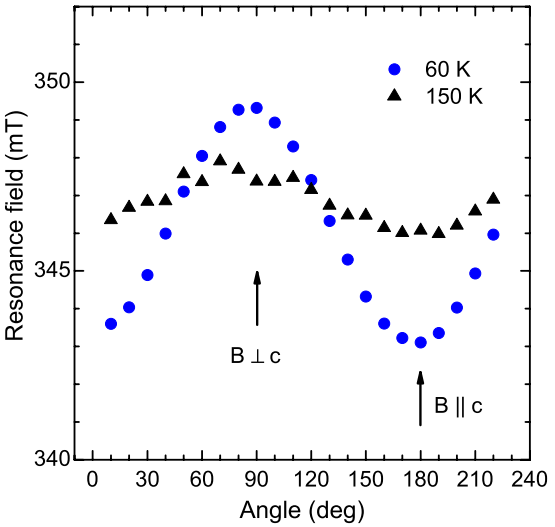

FIG. 8. (Color online) Angular dependence of the resonance field B_{res} at 60 and 150 K. Magnetic field directions parallel and perpendicular to the c axis are indicated by the arrows.

Above 100 K ΔB scales linearly with the temperature T as $\Delta B = A + B \cdot T$, where $A = 142.7$ mT is the residual width and $B = 0.11$ mT/K is the so-called Korringa slope. The term A usually comprises several contributions, such as an unresolved fine-structure, dipolar- and anisotropic exchange interactions as well as structural disorder.[23] The presence of the $B \cdot T$ term suggests that the dominant relaxation channel for Eu spins at high temperatures is due to the spin-flip scattering on conduction electrons, which is a usual relaxation mechanism of the localized spins in metals (Korringa mechanism).[24,25] A superlinear decrease in ΔB below ~100 K indicates an enhancement of ferromagnetic correlations, which yields an additional narrowing of the ESR line by a factor of $\chi^{\mathrm{Curie}}(T)/\chi^{\mathrm{CW}}(T)$.[25] Here χ^{Curie} is the Curie susceptibility of noninteracting spins and χ^{CW} is the susceptibility enhanced due to ferromagnetic spin-spin interactions. This finding is corroborated by the development of the anisotropy of the resonance field in the same temperature range (Fig. 8). Above ~100 K B_{res} depends only slightly on the angle between the magnetic field vector and the hexagonal c axis. This variation may be attributed to a small anisotropy of the g factor, which could arise due to the crystal-field-induced admixture of the high-energy multiplet with a nonzero orbital momentum to the spin-only ground state of Eu^{2+}.[21] However, at lower temperatures the anisotropy of B_{res} substantially increases (Fig. 8) suggesting the emergence of anisotropic magnetization in the sample due to the development of ferromagnetic correlations. In fact, this finding agrees well with the observation of large negative magnetoresistance in a similar temperature range that is also suggestive of appreciable ferromagnetic correlations far above the ordering temperature T_C (see Sec. III D and Ref. 4).

The development of the above-discussed features of ΔB and B_{res} is followed by a substantial transformation of the ESR spectrum upon entering the LT regime (Fig. 9). Here, below 50 K, the signal splits into two components due to the emergence of two magnetically nonequivalent Eu sites that experience different local internal fields as suggested in Ref. 4. The line splitting grows with decreasing the temperature and below the ferromagnetic order transition at $T_C = 34$ K a third line nucleates in the spectrum. The multiline structure if the ESR spectrum can be tentatively assigned to the formation of magnetic domains in this temperature range[23] though its precise nature remains to be elucidated. Finally, below ~10 K the spectrum transforms into a broad asymmetric peak strongly shifted to small fields that can be attributed to a single-mode ferromagnetic resonance response. Note that the LT region identified in the ESR data as a region where the short-range order begins to develop corresponds well to the temperature range where the specific-heat data reveal substantial changes in the magnetic entropy whereas this temperature regime is not clearly seen in the static magnetization data as well as in the ESR intensity.

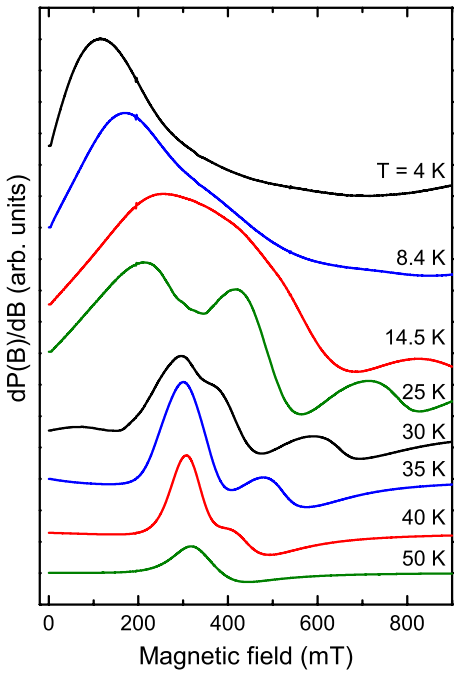

FIG. 9. (Color online) Evolution of the ESR spectra in the LT regime below 50 K (see the text).

D. Electronic transport properties

The electrical resistivity vs temperature $\rho(T)$ at different magnetic fields of single-crystalline samples for the two different a- and c-axis orientations is shown in Fig. 10. The plots have been normalized to the resistance at $T = 295$ K. The absolute value of resistivity $\rho(295\ \mathrm{K}) \sim 285\ \mu\Omega\,\mathrm{cm}$ parallel to the a axis has been reproduced for different samples and after various cooling cycles down to 4.2 K. For samples cut parallel to the c axis an arbitrary resistivity increment was observed on reheating after several cooling cycles. We assume that microcracks within the specimen are responsible for this behavior. However, the temperature dependence of the normalized electrical resistivity $\rho(T)/\rho(295\ \mathrm{K})$ is virtually unaffected by this deficiency, and the lowest absolute resistivity value $\rho(295\ \mathrm{K}) \approx 290\ \mu\Omega\,\mathrm{cm}$ obtained by measurements at different samples was close to that measured along the a axis at zero

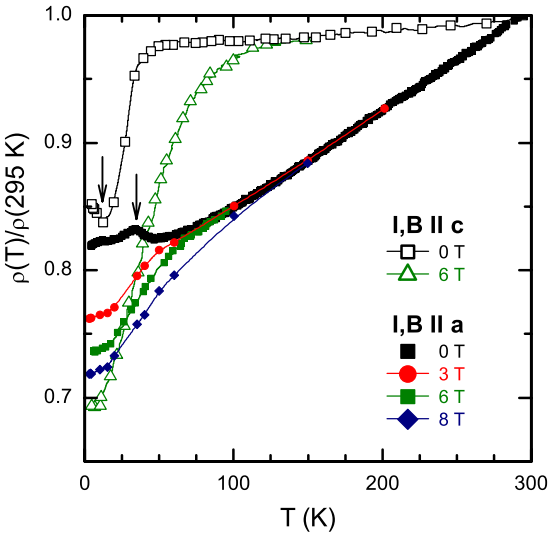

FIG. 10. (Color online) Normalized electrical resistivity $\rho(T)/\rho(295\ \mathrm{K})$ parallel to a and c axes of the Eu_2CuSi_3 single crystal as a function of temperature, longitudinal magnetoresistance for $H\|c$ at $\mu_0 H=6$ T and longitudinal magnetoresistance for $H\|a$ at $\mu_0 H=0$, 3, 6, and 8 T. The solid and dashed arrows indicate resistance anomalies caused by the ferromagnetic transition at $T_C=34$ K and the spin reorientation at low temperature $T\approx 10$ K, respectively.

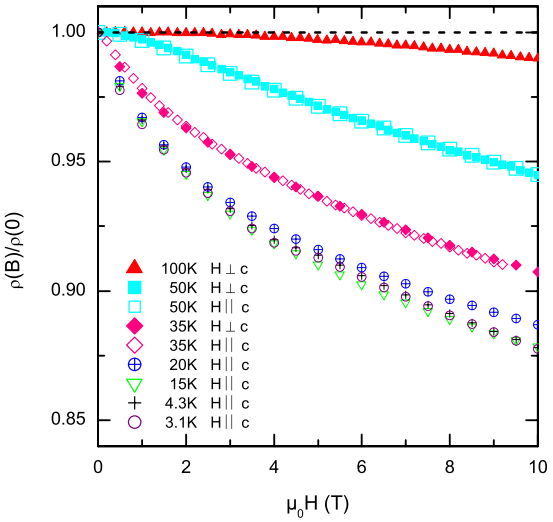

FIG. 11. (Color online) Normalized electrical resistivity of a Eu_2CuSi_3 single crystal parallel to c axis as function of the longitudinal ($H\|c$, open symbols) and transversal ($H\perp c$, filled symbols) external magnetic field for various temperatures $T=3.1-100$ K.

magnetic fields. The temperature dependence of the normalized electrical resistivity $\rho(T)/\rho(295\ \mathrm{K})$ basically reflects metallic behavior but the resistivity drop is smaller than in another Eu bearing compound $EuCu_2Si_2$.[17,26] There is a significant anisotropy for the two different crystallographic orientations. A sudden drop in the electrical resistivity occurs parallel to the c axis near $T_C\approx 34$ K, similar to the findings in polycrystalline samples.[4] However, different from polycrystals, the electrical resistivity parallel to the a axis exhibits a cusp at this temperature, which indicates the ferromagnetic ordering transition. A small anomaly of the resistivity along the a axis is also visible near $T\approx 10$ K (dashed arrow in Fig. 10) concomitant with a rise in resistivity parallel to the c axis. This resistance anomaly is obviously connected with the change in the spin reorientation in the ordered phase discussed in the previous sections.

Below $T\approx 100$ K the resistance is reduced by a longitudinal external magnetic field (Fig. 10). This large negative magnetoresistance is related to the presence of ferromagnetic correlations far above the Curie temperature T_C.[4] The magnetoresistance as function of the external magnetic field for selected temperatures is visualized in Fig. 11. The magnetoresistance $\rho(B)/\rho(0)$ decreases monotonously with increasing field. The dependence in the longitudinal and the transverse field is nearly identical. Even in the highest accessible field of $\mu_0 H=10$ T, $\rho(B)$ does not yet saturate. Remarkably, a significant negative magnetoresistance is already observed at a temperature $T\leq 150$ K, which is much larger than the Curie temperature. With decreasing temperature the negative magnetoresistance increases until it becomes nearly temperature independent at about 12 K. At high fields of 6 T and low temperatures ($T=4.2$ K) the magnetoresistance can exceed 9% for the current parallel to the rod a axis and 20% for the current parallel to the c axis.

IV. DISCUSSION

The Eu_2CuSi_3 compound exhibits ferromagnetic ordering with a significant anisotropy below the $T_C=34$ K. The Curie temperature determined for single crystals is slightly less than $T_C=37$ K found for polycrystals,[4] which is attributed to the stoichiometry deviations within the finite homogeneity range of the R_2TSi_3 compounds.[10,17] The c axis represents the easy magnetic axis. Interestingly, the anisotropy practically disappears when the material undergoes a spin reorientation at $T\sim 10$ K. In polycrystalline Eu_2CuSi_3 samples the orientation dependence of magnetic properties cannot be deduced explicitly, however, a small peak in the magnetic susceptibility below T_C was reported at $T\approx 5$ K, which hints to some anomaly, too.[4]

An analysis of the specific-heat data indicates significant magnetic entropy changes above the magnetic-ordering temperature T_C, which confirms the assumption of considerable short-range magnetic order as supposed by Majumdar *et al.*[4] Moreover, clear signatures of pronounced ferromagnetic quasistatic correlations between Eu moments and the development of the magnetic anisotropy are revealed by ESR at temperatures $T<100$ K far above T_C. As it follows from the analysis of the angular dependence of the resonance field B_{res} of the ESR line in Sec. III C the magnitude of the variation in B_{res} in this temperature regime is substantially larger compared to a very small single-ion anisotropy expected for isolated Eu^{2+} ions. This suggests a collective nature of the magnetic anisotropy of the Eu spin system which develops short-range magnetic correlations below 100 K. Remarkably, the value of B_{res} for the direction of the external field B parallel to the c axis of the single crystal is smaller as compared to the perpendicular geometry. This implies that the effective internal field in the short-range-correlated regions is parallel to the c axis and adds to the external field thus decreasing the value of B_{res}. This result gives complimentary evidence for an easy-axis character of magnetic anisotropy in Eu_2CuSi_3.

The development of ferromagnetic correlations at elevated temperatures suggested by ESR results may explain the occurrence of a large negative magnetoresistance not only in the vicinity but also far above T_C, an observation of some importance for the search of novel systems, which display giant magnetoresistance near room temperature.

Similar to another AlB_2-derived compound, Eu_2PdSi_3,[3] the Eu ions are in a divalent Eu^{2+} state and differ from the mixed valence state in $EuCu_2Si_2$ for instance.[17,26] At temperatures $T<50$ K the ESR signal splits into two components due to the emergence of two magnetically nonequivalent Eu sites, which are also evidenced by Mössbauer measurements at $T<T_C$, where magnetic hyperfine split spectra could only be fitted with the assumption of two sites.[4] The two magnetic transitions at $T_C=34$ K and $T\approx 10$ K observed may be attributed to nonequivalent Eu sites. The local modification of Eu sites turns out to be more distinct for Eu_2PdSi_3 where evidence for an antiferromagnetic component was found below 10 K.[3] The study of Eu_2PdSi_3 single crystals is the subject of future work.

V. CONCLUSIONS

Summarizing, the presented results of magnetization, specific heat, and electrical resistivity studies on Eu_2CuSi_3 single crystals support ferromagnetic ordering at $T_C=34$ K. According to magnetization measurements the magnetic anisotropy is sizable at $T<T_C$ and the c axis is identified as the easy magnetic axis. Remarkably, below $T\approx 10$ K the magnetic anisotropy almost vanishes most probably due to a spin reorientation as suggested by the analysis of the specific-heat data. The anisotropy of the resonance field and the additional narrowing of the electron-spin resonance line of Eu^{2+} ions at $T<100$ K prove appreciable short-range ferromagnetic correlations far above T_C. These can explain the occurrence of a large negative magnetoresistance even up to temperatures $T\sim 100$ K. Below 50 K the electron-spin resonance line starts to split due to the emergence of two magnetically nonequivalent Eu sites. Upon entering the magnetically ordered state a third line emerges in the spectrum. Finally, the spectrum transforms into a broad asymmetric peak below $T\approx 10$ K which correlates with a transition from an anisotropic to an isotropic spin state as suggested by the specific-heat measurements.

ACKNOWLEDGMENTS

The authors thank S. Pichl, S. Mueller-Litvanyi, J. Werner, and R. Müller for experimental assistance and for helpful discussions. Some authors express their gratitude to financial support by SFB 463 of the Deutsche Forschungsgemeinschaft (W.L. and G.B.), the Alexander von Humboldt-Stiftung, the NSFC (Grant No. 50871088) and NPU-FIST (C.D.C.).

[1] P. A. Kotsanidis, J. K. Yakinthos, and E. Gamari-Seale, J. Magn. Magn. Mater. **87**, 199 (1990).
[2] A. Szytula, M. Hofmann, B. Penc, M. Slaski, S. Majumdar, E. V. Sampathkumaran, and A. Zygmunt, J. Magn. Magn. Mater. **202**, 365 (1999).
[3] R. Mallik, E. V. Sampathkumaran, M. Strecker, G. Wortmann, P. L. Paulose, and Y. Ueda, J. Magn. Magn. Mater. **185**, L135 (1998).
[4] S. Majumdar, R. Mallik, E. V. Sampathkumaran, K. Rupprecht, and G. Wortmann, Phys. Rev. B **60**, 6770 (1999).
[5] S. M. Dhar, R. Balasubramanium, S. M. Pattalwar, and R. Vijayaraghavan, J. Alloys Compd. **210**, 339 (1994).
[6] J. S. Hwang, K. J. Lin, and C. Tien, Solid State Commun. **100**, 169 (1996).
[7] E. V. Sampathkumaran, I. Das, R. Rawat, and S. Majumdar, Appl. Phys. Lett. **77**, 418 (2000).
[8] S. R. Saha, H. Sugawara, T. D. Matsuda, H. Sato, R. Mallik, and E. V. Sampathkumaran, Phys. Rev. B **60**, 12162 (1999).
[9] S. R. Saha, H. Sugawara, T. D. Matsuda, Y. Aoki, H. Sato, and E. V. Sampathkumaran, Phys. Rev. B **62**, 425 (2000).
[10] G. Behr, W. Löser, G. Graw, H. Bitterlich, J. Fink, and L. Schultz, Cryst. Res. Technol. **35**, 461 (2000).
[11] G. Graw, H. Bitterlich, W. Löser, G. Behr, J. Fink, and L. Schultz, J. Alloys Compd. **308**, 193 (2000).
[12] S. Majumdar, E. V. Sampathkumaran, P. L. Paulose, H. Bitterlich, W. Löser, and G. Behr, Phys. Rev. B **62**, 14207 (2000).
[13] S. Majumdar, H. Bitterlich, G. Behr, W. Löser, P. L. Paulose, and E. V. Sampathkumaran, Phys. Rev. B **64**, 012418 (2001).
[14] I. Mazilu, M. Frontzek, W. Löser, G. Behr, A. Teresiak, and L. Schultz, J. Cryst. Growth **275**, e103 (2005).
[15] M. Frontzek, A. Kreyssig, M. Doerr, M. Rotter, G. Behr, W. Löser, I. Mazilu, and M. Loewenhaupt, J. Magn. Magn. Mater. **301**, 398 (2006).
[16] G. Behr, W. Löser, D. Souptel, G. Fuchs, I. Mazilu, C. Cao, A. Köhler, L. Schultz, and B. Büchner, J. Cryst. Growth **310**, 2268 (2008).
[17] C. D. Cao, R. Klingeler, N. Leps, H. Vinzelberg, V. Kataev, F. Muranyi, N. Tristan, A. Teresiak, S. Q. Zhou, W. Löser, G. Behr, and B. Büchner, Phys. Rev. B **78**, 064409 (2008).
[18] C. N. Wizent, L. Schramm, G. Behr, W. Löser, W. Gruner, A. Voß, B. Büchner, and L. Schultz, J. Solid State Chem. **182**, 2036 (2009).
[19] R. Klingeler, J. Geck, R. Gross, L. Pinsard-Gaudart, A. Revcolevschi, S. Uhlenbruck, and B. Büchner, Phys. Rev. B **65**, 174404 (2002).
[20] F. J. Dyson, Phys. Rev. **98**, 349 (1955).
[21] A. Abragam and B. Bleaney, *Electron Paramagnetic Resonance of Transition Ions* (Oxford University Press, London, 1970).
[22] G. Michels, M. Roepke, T. Niemöller, M. Chefki, M. M. Abd-Elmeguid, H. Micklitz, E. Holland-Moritz, W. Schlabitz, C. Huhnt, B. Büchner, A. Wurth, A. Mewis, and V. Kataev, J. Phys.: Condens. Matter **8**, 4055 (1996).
[23] S. E. Barnes, Adv. Phys. **30**, 801 (1981).
[24] J. Korringa, Physica (Amsterdam) **16**, 601 (1950).
[25] D. L. Huber, J. Phys. Chem. Solids **32**, 2145 (1971).
[26] P. G. Pagliuso, J. L. Sarrao, J. D. Thompson, M. F. Hundley, M. S. Sercheli, R. R. Urbano, C. Rettori, Z. Fisk, and S. B. Oseroff, Phys. Rev. B **63**, 092406 (2001).